



Enzymatic synthesis of 4-methoxycinnamoylglycerol Uv filter mediated by immobilized-lipase and nanoparticle formation on N-succinylchitosan

Síntesis enzimática del filtro UV 4-metoxicinamoilglicerol mediado por lipasa inmovilizada y formación de nanopartículas N-succinilquitosano

Sindy Escobar¹; Claudia Bernal²; Mónica Mesa^{3*}

¹Química Farmacéutica, Ph.D. Universidad de Antioquia - UdeA, Grupo Ciencia de los Materiales, Instituto de Química, Facultad de Ciencias Exactas y Naturales. Medellín - Antioquia, Colombia; e-mail: sindy503@gmail.com; <http://orcid.org/0000-0002-7247-119X>

²Química, Ph.D. Universidad de La Serena, Escuela de Ingeniería de Alimentos, Tecnología Enzimática para Bioprocesos. La Serena, Chile; e-mail: clabertz@gmail.com; <http://orcid.org/0000-0001-9117-0483>

³Química, Ph.D. Ciencias Químicas. Universidad de Antioquia - UdeA, Facultad de Ciencias Exactas y Naturales, Instituto de Química, Grupo Ciencia de los Materiales. Medellín - Antioquia, Colombia; e-mail: monica.mesa@udea.edu.co <http://orcid.org/0000-0002-6175-6384>

*autor para correspondencia: monica.mesa@udea.edu.co

How to cite: Escobar, S.; Bernal, C.; Mesa, M. 2020. Enzymatic synthesis of 4-methoxycinnamoylglycerol Uv filter mediated by immobilized-lipase and nanoparticle formation on N-succinylchitosan. Rev. U.D.C.A Act. & Div. Cient. 23(2):e1631. <http://doi.org/10.31910/rudca.v23.n2.2020.1631>

Open access article published by Revista U.D.C.A Actualidad & Divulgación Científica, under Creative Commons License CC BY-NC 4.0

Official publication of the Universidad de Ciencias Aplicadas y Ambientales U.D.C.A, University, Accredited as a High-Quality Institution by the Colombian Ministry of Education.

Received: July 7, 2020 **Accepted:** November 27, 2020 **Edited by por:** Ingeborg Zenner de Polanía

ABSTRACT

The synthesis of 4-methoxycinnamoylglycerol takes advantage of the biodiesel subproduct for obtaining a hydrophilic UV cinnamate derivate filter, useful in sunscreen formulations. The objective here was to demonstrate that esterification of 4-methoxycinnamic acid and glycerol mediated by immobilized-lipase from *Thermomyces lanuginosus* is selective towards 4-methoxycinnamoylglycerol monoester UV filter, whose chemical characteristics favor the nanoparticles formation by ionotropic gelation on N-Succinyl chitosan. A cinnamic acid conversion ~34% in hexane is higher than in other reports, without the presence of other sub-products or degradation products. This eases the purification process by liquid-

liquid extraction. The free glyceryl entities favour its incorporation on N-Succinyl chitosan nanoparticles with size around 185 ± 77 nm, which are promissory for sunblock products.

Keywords: Cinnamate derivatives; UV radiation filter; Nanoparticles; Immobilized lipases (Fragments found in Mesh Browser).

RESUMEN

En la síntesis de 4-metoxicinamoilglicerol, se aprovecha el subproducto de biodiesel para obtener un filtro UV hidrofílico, derivado de cinamato, útil en formulaciones de bloqueadores solares. El objetivo de este trabajo fue demostrar que la esterificación del ácido

4-metoxicinámico y el glicerol, mediado por la lipasa inmovilizada de *Thermomyces lanuginosus*, es selectiva hacia el monoéster del filtro UV 4-metoxicinamoylglicerol, cuyas características químicas favorecen la formación de nanopartículas, por gelificación ionotrópica en N-succinil-quitosano. Una conversión de ácido cinámico ~34% en hexano es mayor que los valores ya reportados, sin la presencia de otros subproductos o productos de degradación. Esto facilita, el proceso de purificación por extracción líquido-líquido. Las entidades de glicerilo libre favorecen su incorporación en nanopartículas de N-succinil-quitosano, con un tamaño de alrededor de 185 ± 77 nm, que son promisorias para los productos de protección solar.

Palabras clave: Derivados de cinnamato; Filtro radiación UV; Nanopartículas; Lipasa inmovilizada.

INTRODUCTION

The cinnamates are UV filters that absorb around 310 nm due to the unsaturated carbons conjugated system and, the presence of a methoxy group broadens the absorption range up to 350 nm (Holser, 2008; Shaath, 2010). A typical example in commercial sunscreens is the octyl methoxy cinnamate (OMC) ester produced from 4-methoxycinnamic acid (4-MCA) and 2-ethyl-hexanol (Lee *et al.* 2006). Changing the lineal alcohol by glycerol leads to the 4-methoxycinnamoylglycerol (4-MCG) ester, which is more hydrophilic than the OMC, widening the range of solubilization vehicles than can be used during the sunscreen formulation, preserving the absorption ability of these cinnamates. The 4-methoxycinnamoylglycerol (4-MCG) is in form of mono- and di-esters when the esterification reaction is carried out in the presence of p-toluenesulfonic acid (p-TSA) (Holser, 2008; Holser *et al.* 2008). An improved conversion yield was reported by enzymatic synthesis using lipase, in addition to the prevalence of the monoester at short reaction times and less harmful side effects compared with the chemical route (Patil *et al.* 2011). It is well-known that lipases act as esterases in non-aqueous reaction media (Bernal *et al.* 2018; Fernandez-Lafuente, 2010), including the esterification of cinnamic acid (Patil *et al.* 2011) and/or glycerol (Yesiloglu & Kilic, 2004) and the obtained products have different industrial applications (Naik *et al.* 2010). The lipase activity and selectivity depend on water activity (Lee & Parkin, 2001) and solvent polarity (Kuo & Parkin, 1996) of the reaction media. Additionally, this selectivity can be modulated by immobilization in solid supports, as reported for different lipases adsorbed in Celite, for which the lipid modifications is selective to the size of the unsaturated carbon chains (Lee & Parkin, 2001). Moreover, their immobilization helps to their implementation at industrial level, allowing the easy recovery from the reaction medium in batch processes and increases the reuse cycles on packed bed continuous bioreactors (Babaki *et al.* 2016). The lipase B from the *Candida antarctica* yeast, immobilized on acrylic resin is commercially available (Novozym 435) and tested for the synthesis of 4-MCG (Patil *et al.* 2011) and other cinnamates (Lee *et al.* 2006) at temperatures between 40 - 60°C.

The lipases from the thermophilic *Thermomyces lanuginosus* fungus is attractive for synthesis of different products through the

esterification reaction, because it is thermophilic and active in a wide pH range (Fernandez-Lafuente, 2010). Its immobilization has improved its catalytic behavior in this kind of reaction due to the interfacial activation (Bassi *et al.* 2016; Zhou *et al.* 2012), thermal and conformational stabilization (Bernal *et al.* 2018; Matte *et al.* 2014) conferred by the support. Moreover, its immobilization by one-pot silica sol-gel process in the presence of polyethylenimine (PEI) is so simple for obtaining a biocatalyst with high protein load (90%), encapsulation yield (47%) and 247-times more stable at 65°C than the soluble enzyme (Escobar *et al.* 2018), which could increase the conversion degree of 4-MCA and glycerol during the esterification reaction at 65°C. This immobilized-lipase has been not tested yet for production of 4-MCG.

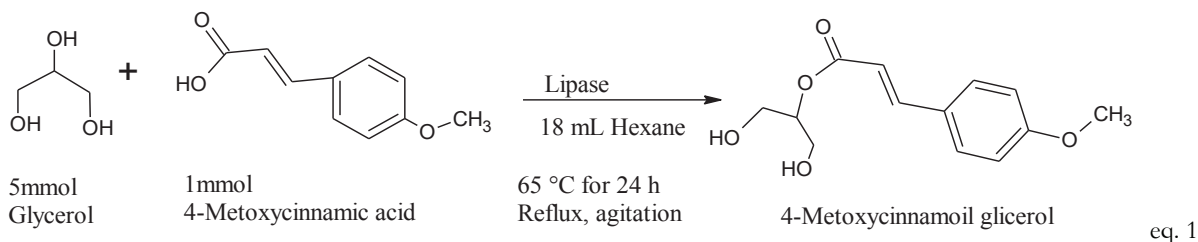
On the other hand, we hypothesized here that the production of 4-MCG in form of nanoparticles could be another advantage for using this UV-filter in the sunscreen formulations. This is inspired in other reports that show the use of nanoparticles in sunscreens (Santos *et al.* 2019), evaluated according to the harmonized safety assessment guides (Katz *et al.* 2015), avoid the UV filters penetration through the skin and systemic cytotoxicity (Nohynek & Dufour, 2012). The free glycerol entities and hydrophilic character of the 4-MCG can be exploited for its incorporation in N-Succinyl-chitosan (NSC) nanoparticles during the ionotropic gelation in the presence of tripolyphosphate (TPP). A low modification degree of NSC (~28%) and mixtures with non-modified chitosan favored the formation of nanoparticle with sizes lower than 160 nm by ionotropic gelation and the purification by Ultrafiltration gave a monodisperse distribution (Monsalve *et al.* 2015). The NSC nanoparticles have been used as carrier of hydrophilic molecules such as encapsulated polyphenols (Palacio *et al.* 2020), grafted catechols (Sahatsapan *et al.* 2019) and lipoproteins (Zhang *et al.* 2014).

The objective of this paper was to demonstrate that esterification of 4-MCA and glycerol mediated by the immobilized-lipase of *T. lanuginosus* is selective towards 4-MCG monoester UV filter, whose chemical characteristics favor its incorporation in nanoparticles, during the ionotropic gelation of NSC.

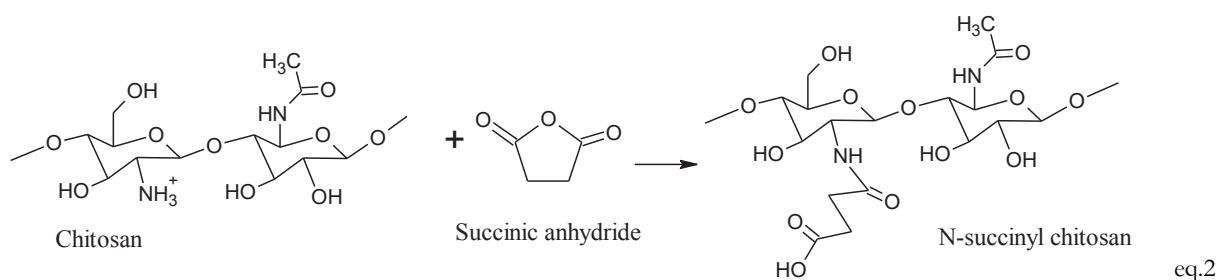
MATERIALS AND METHODS

Esterification reaction. This was carried out by enzymatic synthesis, using the immobilized-lipase biocatalyst prepared by the one-pot silica/PEI sol-gel strategy (0.4 mg mL⁻¹ of lipase with 1300 - 1700 U mL⁻¹, 3.1 wt% PEI, pH 5.5, 50°C, 24h) (Escobar *et al.* 2018). Before its use, its kinetic parameters (Michaelis-Menten constant, Km and maximum velocity, Vmax) and diffusion restrictions were measured by p-NPB and fluorescein dilaurate tests, respectively (Soto *et al.* 2017) and reported respecting to the soluble enzyme (Km = 4.92 mM, and Vmax = 8.03 mM min⁻¹).

The esterification between dry glycerol and 4-MCA (5:1 mmol ratio) was made in hexane or t-amyl alcohol (18 mL) at 65°C (reflux) in the presence of 7 mg of the immobilized-lipase, under magnetic agitation for 24h (eq. 1).



At the end, the liquid phase (that contains the reaction products) was separated from the biocatalyst by filtration. Both phases were characterized by different methods, described below. A partial purification of the produced esters from unreacted 4-MCA was carried out by liquid-liquid extraction, by using carbonate solution before to be submitted to characterization by HPCL, FTIR, ^{13}C -NMR and UV-Vis analysis. The same esterification reaction was made in the presence of p-TSA (Holser, 2008) instead of the enzyme for making comparisons.



Then, 50mg of this NSC derivate in water (30mL) was put in contact with 4-MCG (12mg) during 24h under magnetic agitation. At the end, the product was dialyzed against water, lyophilized and characterized by FTIR.

After that, 5mg of this powder was dissolved in 1% acetic acid (5mL) by sonication during 1min (10 s ON and 10 s OFF, amplitude 90%), pH raising up to 5.0 and sonication under the same conditions. The triphosphosphate (TPP) dissolved in miliQ water (1mg/mL, pH 7.0) was added at 25°C, varying the weight ratio for modulating the nanoparticle size and its distribution. The samples were purified by ultrafiltration (1kDa cellulose membrane) and centrifugation at 4000rpm for 10min before the characterization by DLS. The quantification of 4-MCG in the nanoparticles was made by Uv-vis spectrometry by using a calibration curve represented by the equation $\text{Abs} = 19483\text{C} + 0.1521$ at 310nm.

Characterization methods. All samples synthesized in this work were analysed by transmittance FTIR in a ZnSe plate in a Perkin Elmer spectrophotometer ($450 - 3500\text{cm}^{-1}$ and 16 scans) for obtaining information about the ester formation between 4-MCA and glycerol, and the obtention of NSC. The chemical identity 4-MCG was corroborated by liquid ^{13}C -NMR (Bruker Ascend III HD 600 MHz spectrometer with 5mm TXI probe) for which, the sample was dissolved in deuterated methanol. The conversion

Preparation of 4-MCG nanoparticles. The incorporation of 4-MCG to NSC was carried out for preparing 4-MCG nanoparticles by ionotropic gelation. The NSC was obtained by the reaction of chitosan acetate (200mg) and succinic anhydride (39mg) in water (30L) under the conditions described by Monsalve *et al.* (2015) (eq. 2), for having a derivate exhibiting ~28% of amine substitution degree and isoelectric point at pH = 7.2.

percentage of 4-MCA to 4-MCG was calculated from HPLC results (Agilent HPLC-DAD/FLD instrument, UV diodes detector, mobile phase methanol: H_2O (70:30), C18 ZORBAX SB 5um, 250mm x 4.6um column). The peak area (for the pure 4-MCA and after reaction) was assumed proportional to the weight percentage of the 4-MCA for making the calculations. The 4-MCG molar extinction coefficient at 310nm was determined from the analysis 4-MCG solutions in methanol (concentrations between 2×10^{-7} to $2 \times 10^{-4}\text{M}$) by UV/Vis spectroscopy (Perkin Elmer model lambda 25 instrument). The same analysis was made for OMC solutions, under similar conditions. The size of 4-MCG-NSC nanoparticles was determined by Dynamic Light Scattering (Horiba LB 550).

The catalytic activity of the immobilized-lipase biocatalyst was measured by p-NPB UV/Vis activity assay (Escobar *et al.* 2018) before and after its use in the 4-MCG synthesis. The preserved (residual) activity was reported as percentage respecting to the initial activity.

RESULTS AND DISCUSSIONS

Esterification of 4-MCA and glycerol mediated by immobilized-lipase solid biocatalyst. The synthesis of 4-MCG was made at 65°C by esterification of 4-MCA and glycerol, catalyzed by immobilized-lipase in non-aqueous solvent. This biocatalyst was

chosen because: (i) its preparation is very simple and reproducible by an one-pot silica/PEI sol-gel strategy (0.4mg mL^{-1} lipase, $3.1\text{ wt}\%$ PEI, $\text{pH } 5.5$, 50°C , 24h); (ii) it is 247-times more stable at 65°C than the soluble enzyme (Escobar *et al.* 2018); (iii) it exhibits higher specific activity (600U g^{-1}) (Escobar *et al.* 2018) than that immobilized by adsorption on mesoporous organosilicas or organic supports (Cipolatti *et al.* 2016); (iv) the solid siliceous solid support allows its easy recovering from the reaction media and the subsequent reuse. This is demonstrated here, retaining around 50% of activity after 4 catalysis cycles in hexane at 65°C (Figure 1a). This has a positive impact in the cost/effective balance of the organic synthetic processes.

On the other hand, the hexane and *t*-amyl alcohol were tested as non-aqueous solvents. The conversion of 4-MCA to 4-MCG, determined from HPLC analysis (Figure 2), is 14-times higher in hexane than in the *t*-amyl alcohol. Although the substrates are more soluble in later solvent, the hexane favors the shift of the hydrolysis-

esterification equilibrium towards the ester formation. It is because its non-polar nature contributes to the lipase interfacial activation, and therefore, the improved interaction of the substrates with the active site of enzyme for their catalytic esterification (Patil *et al.* 2011; Bastida *et al.* 1998).

The HPLC chromatogram for the sample obtained after esterification in hexane at 65°C by using the immobilized-lipase exhibits a major component (retention time $\sim 3\text{min}$), well-solved from other traces peaks. In contrast, the sample prepared in the presence of *p*-TSA as catalyst and keeping constant the other parameters (including the HPLC analysis conditions), has a more complex chromatogram (Figure 2a). The relative contribution of the peak $\sim 3\text{min}$, corresponding to 4-MCG, is more important in the sample prepared in the presence of the enzyme (78.56%) than with *p*-TSA (8.14%), even some 4-MCA and solvent traces could be present in both cases.

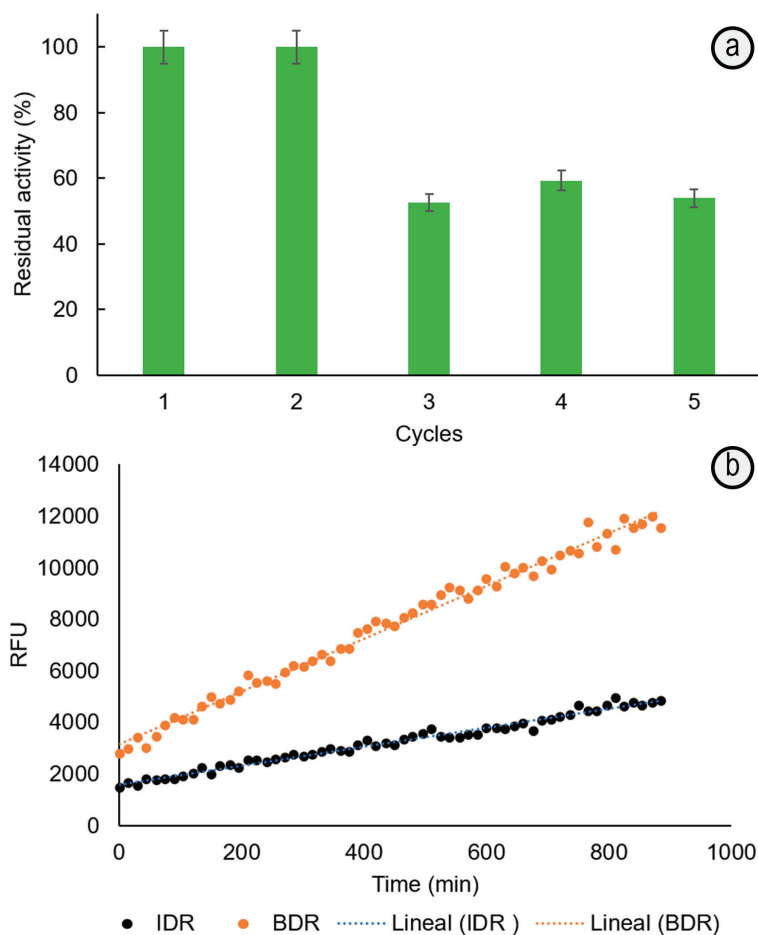


Figure 1. a. Reuse assay of immobilized-lipase biocatalyst in hexane at 65°C . The catalytic activity measured by *p*-NPB test. b. Diffusion test: Relative Fluorescence Units per minute (RFU, measured by Confocal Microscopy) from 0.1mM fluorescein dilaurate hydrolysis in the bulk ($\text{BDR} = 10.4 \pm 0.7\text{RFU min}^{-1}$) and into the particles with immobilized-lipase ($\text{IDR} = 3.6 \pm 0.1\text{RFU min}^{-1}$, average from 10 particles). All measurements were made by duplicate and the corresponding standard deviations are indicated.

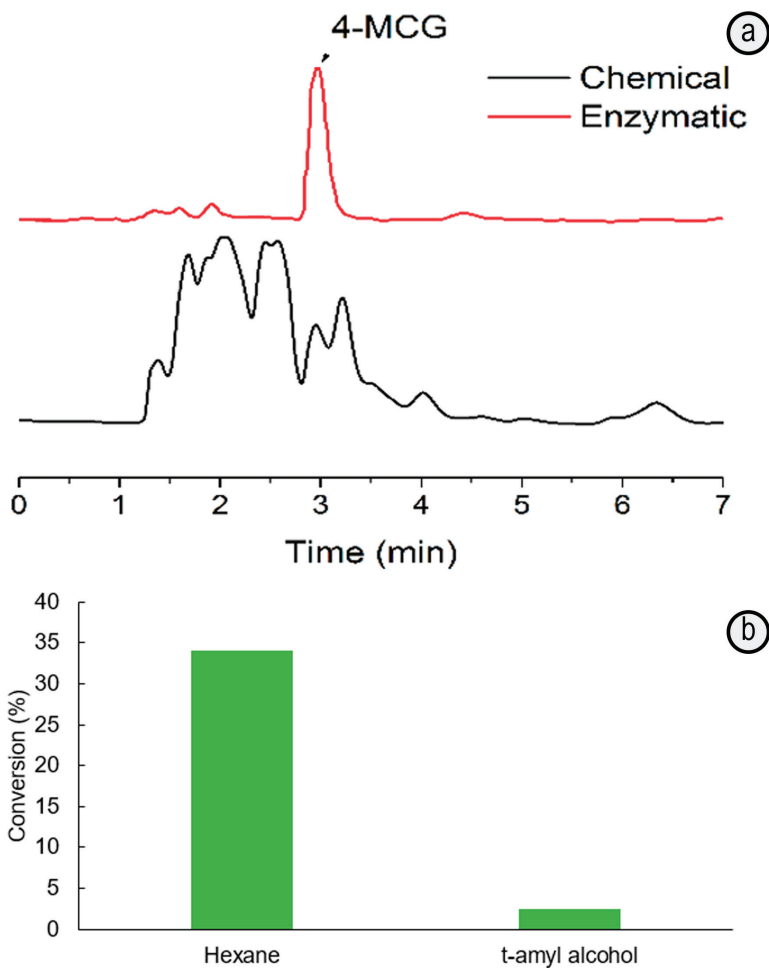


Figure 2. HPLC chromatograms for samples obtained by esterification of 4-MCA and glycerol mediated by p-TSA (Chemistry synthesis) or immobilized-lipase (Enzymatic synthesis) in hexane at 65°C. a. Conversion degree of 4-MCA into 4-MCG mediated by immobilized-lipase biocatalyst at 65°C in hexane or t-amyl alcohol; b. The data were obtained by triplicated and the significant difference evaluated with ANOVA test at $\alpha=0.05$.

The chemical characterization of both samples by FTIR after purification by liquid-liquid extraction in the presence of carbonate solution (Holser *et al.* 2008) (Figure 3a) indicates the ester formation by the presence of carbonyl (-COOR) signals at 1700cm^{-1} , which is shift to 1740cm^{-1} due to the presence of the unsaturated and aromatic carbon conjugated system (Holser, 2008) and C-O stretches in the $1300\text{-}1000\text{cm}^{-1}$. The band at 1688cm^{-1} , typical of -COOH group in the cinnamic acid (Patil *et al.* 2011; Ferenc *et al.* 2012), disappears in the sample synthesized by the enzymatic pathway. Meanwhile, it is still contributing to the widening of the band centered around 1700cm^{-1} in the sample prepared with p-TSA (Figure 3a). This can be correlated with the higher consumption degree of the 4-MCA in the reaction mediated by the immobilized-lipase compared with that in the presence of p-TSA. The FTIR spectra also show the band at $3200\text{-}3600\text{cm}^{-1}$ (Figure 3a) corresponding to hydroxyls, which comes mainly from the glyceryl groups (Patil *et al.* 2011).

The signals of the ^{13}C -NMR spectrum corroborate the ester formation by the shift at 171.0ppm (Figure 3b), characteristic

of C=O ester bond (Sun *et al.* 2013). There is also a chemical shift at 178.0ppm of C=O bond of carboxyl acid, possibly, due to the presence cinnamic acid traces, evidenced in the HPLC chromatogram (Figure 2a).

These results indicate that the use of the immobilized-lipase biocatalyst avoids the formation of several by-products (such as monoester, diester, triester, degradation products), commonly found in the esterification of glycerol and cinnamic acid derivatives in the presence of p-TSA (Holser, 2008; Lee *et al.* 2006).

The monoester could be formed through the primary hydroxyl, favored by the short reaction time (Holser *et al.* 2008), specificity and hyperactivation of the immobilized-lipase from *T. lanuginosus* in non-aqueous solvents (Bassi *et al.* 2016; Fernandez-Lorente *et al.* 2008). Moreover, the decrease of the immobilized-lipase affinity and maximum reaction velocity for substrates such as p-NPB (1.88- and 0.88-times higher K_m and lower V_{max} , respectively than for the soluble one) indicate that esterification product can be less prone to

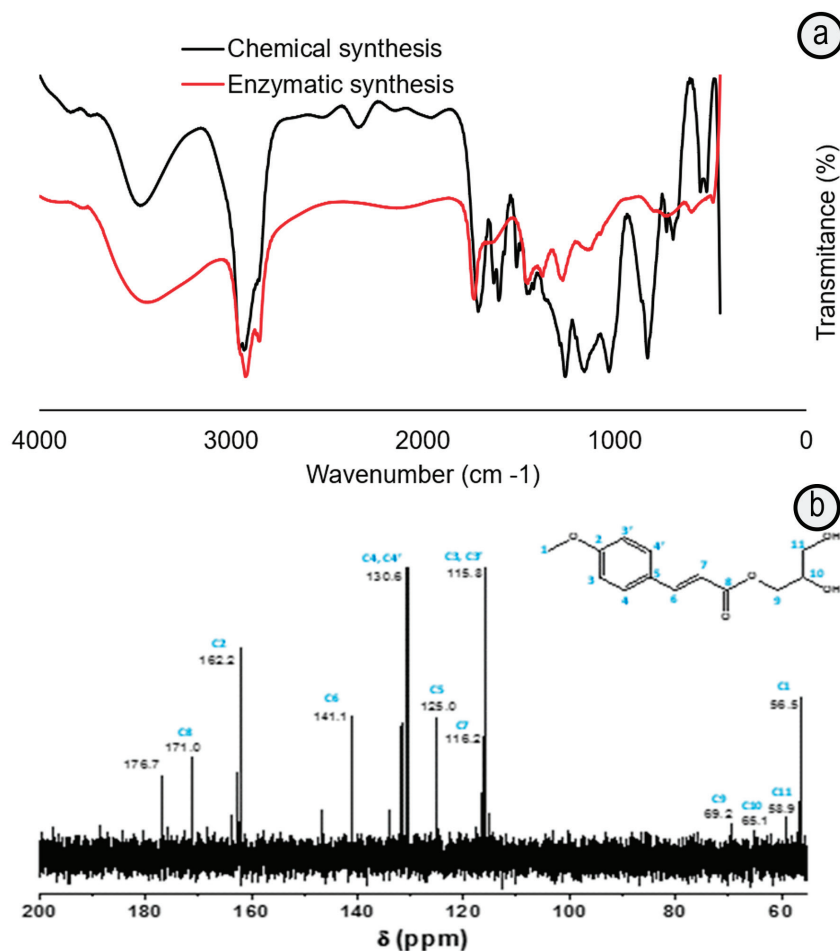


Figure 3. FTIR a. and ¹³C NMR b. spectra of samples obtained by esterification of 4-MCA and glycerol mediated by immobilized-lipase biocatalyst (Enzymatic) or p-TSA (Chemical) in hexane at 65°C and purified by liquid-liquid extraction.

hydrolysis and formation of degradation products during the reaction time. The morphology, porosity and composition of the solid matrix make difficult the substrate mass transfer towards immobilized-lipase and, contributing also to the lowering of the hydrolysis rate. The Bulk/Intraparticle hydrolysis rates ratio > 1 (Figure 1b), measured from a confocal microscopy diffusion experiment, point out the mass transfer restrictions imposed by the solid support. These have consequences on the substrate interactions in the active site (Cipolatti *et al.* 2016; Soto *et al.* 2017) of the immobilized-lipase and therefore, affects the K_m and V_{max} kinetic parameters. The important thing in this work is that the tortuosity of the solid matrix could also hinder the formation of bigger by-products (diester, triester) or at least, lowering their diffusion up to the bulk solution. The presence of almost a unique product, with a higher conversion degree compared with that obtained by using *C. antarctica* lipase B (Novozym 435, immobilized on acrylic resin) as catalyst (Patil *et al.* 2011) allow a simple and faster purification process.

Absorption properties of 4-MCG and nanoparticle formation with N-succinyl-chitosan. The UV spectrum of 4-MCG was measured between 200-400nm (Figure 4), showing three main absorption bands in a wide UVB region (240-340nm), like those

observed for the OMC molecule (Hanson *et al.* 2015). These bands are associated with transition $\pi-\pi^*$ in the near UV range. The molar extinction coefficient (ϵ) for 4-MCG at 310nm was 19483 M⁻¹cm⁻¹. This value is higher than that measured for the OMC ($\epsilon=12600$ M⁻¹cm⁻¹), indicating a higher quantum efficiency of the 4-MCG. Taking into account that the ϵ_{4-MCG} is in the range of values reported for other molecules used as UV filters (Shaath, 2010), the 4-MCG can be promissory for being used in sunscreen formulations, with the advantages of having glyceryl functional groups in its structure (Patil *et al.* 2011). They confer a higher hydrophilic character to the 4-MCG compared with the OMC, lowering the skin permeability, which can help to avoid systemic toxicity associated to the absorption of some sunscreen active ingredients (Nohynek & Dufour, 2012). On the hand, the hydrophilicity allows its incorporation on NSC nanoparticles, which call the attention for cosmetic formulations (Santos *et al.* 2019).

In this case, the NSC was obtained by modification of chitosan with succinic anhydride. The FTIR spectrum (Figure 5) exhibits new bands at 1576cm⁻¹ and 1465cm⁻¹ from the amide II and -COOH symmetric stretching vibrations, which evidence the formation of NSC (Palacio *et al.* 2020; Sahatsapan *et al.* 2019). The absorption

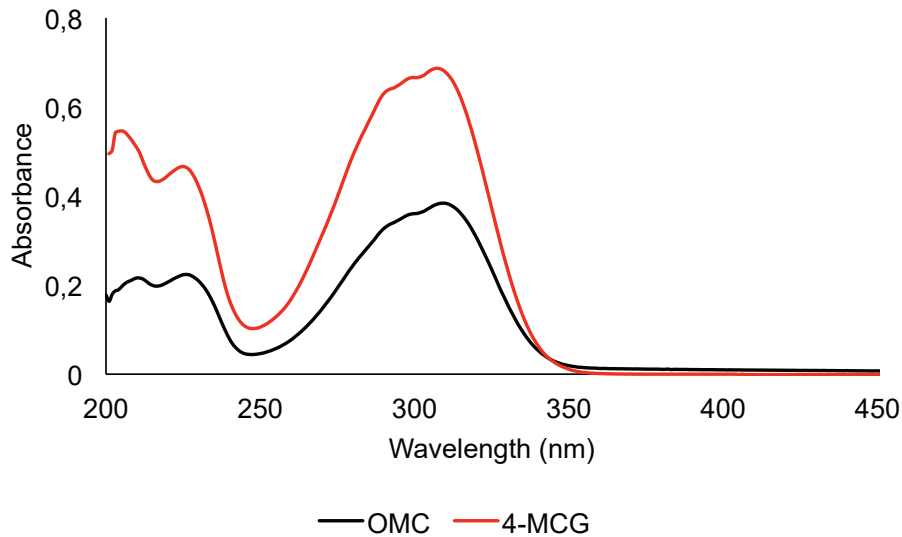


Figure 4. UV spectra of 4-methoxycinnamoylglycerol (4-MCG) and Octylmethoxycinnamate (OMC) measured in methanol.

peaks at 1632cm^{-1} , 1512cm^{-1} , and 1385cm^{-1} can be attributed to band amide I, with the presence of the C=O stretching. The band at 1154cm^{-1} corresponds the stretching of C-O-C and the band at 1090cm^{-1} involved the C-O stretching.

The nanoparticles were prepared through ionotropic gelation method, varying the NSC:TPP weigh ratio (Table 1). The size of the nanoparticles decreased when the TPP concentration was increased, due to the increased cross-linking of the polymer. The NSC:TPP ratio equal to 1:1 lead to nanoparticles with the narrower nanoparticle size around 185nm. These are a little bigger than those

obtained with NSC by ionotropic gelation (160nm) (Monsalve *et al.* 2015) because of the presence of 4-MCG. This preserved the UV absorption ability, because the aromatic ring is not affected during the polymer crosslinking. The incorporation degree was around $16.1\pm 4.5\%$ and there is not a significant variation when the TPP was changed, showing that it is more dependent on the interaction of the 4-MCG with the NSC before the formation of the nanoparticles, whose conditions were kept constant for all the samples. These 4-MCG/NSC interactions proceed through the protonated amines remaining on the NSC ($\sim 28\%$ of substitution degree).

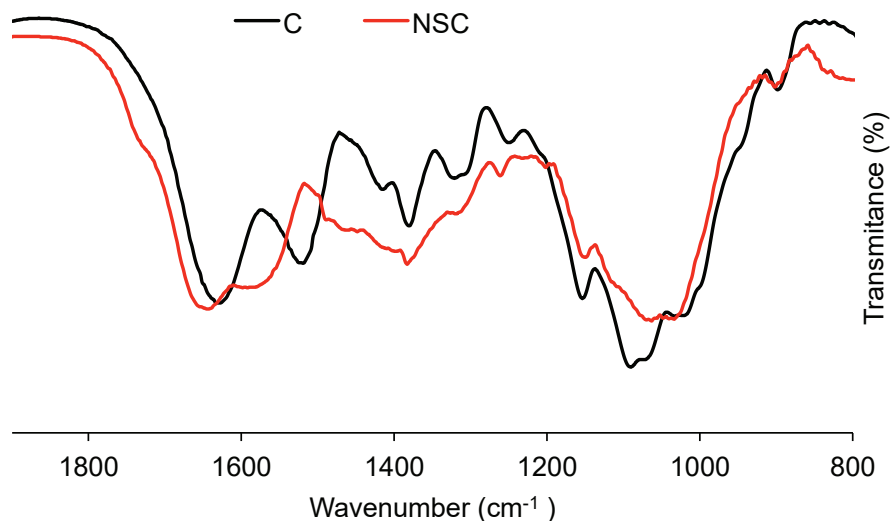


Figure 5. FTIR spectra of chitosan (C, MW 148.985 Da; %DD 76) and N-Succinyl chitosan (NSC).

Table 1. Size of nanoparticles prepared by ionotropic gelation method with N-succinyl chitosan-4MCG and TPP at 25°C and pH 5.0. (Samples obtained by triplicated, size reported as mean \pm standard deviation). Significant differences evaluated with ANOVA test at $\alpha=0.05$.

NSC:TPP weight ratio	Size (nm)
50:1	2077 \pm 773
2:1	722 \pm 209
1:1	185 \pm 77

In conclusion, the immobilized-lipase from *T. lanuginosus*, exhibiting high activity and thermal stability, allowed the esterification reaction of 4-methoxycinnamic acid and glycerol, at 65°C in hexane. It was a clean pathway, reaching ~34% substrate conversion, and the reuse of the solid biocatalyst from the reaction media. This allowed simplifying the purification process.

The free glyceryl entities conferred hydrophilicity to the 4-methoxycinnamoylglycerol product. This favoured its incorporation on N-succinylchitosan and promoted the formation of nanoparticles with size around 185 \pm 77nm by ionotropic gelation. The UV absorption capacity of 4-Methoxycinnamoylglycerol in form of nanoparticles is promissory for sunscreens formulations.

Conflicts of interest: The manuscript was prepared and revised by all authors, who declare the absence of any conflict which can put the validity of the presented results in risk.

REFERENCES

- BABAKI, M.; YOUSEFI, M.; HABIBI, Z.; MOHAMMADI, M.; YOUSEFI, P.; MOHAMMADI, J.; BRASK, J. 2016. Enzymatic production of biodiesel using lipases immobilized on silica nanoparticles as highly reusable biocatalysts: effect of water, t-butanol and blue silica gel contents. *Renewable Energy*. 91:196-206. <https://doi.org/10.1016/j.renene.2016.01.053>
- BASSI, J.J.; TODERO, L.M.; LAGE, F.A.P.; KHEDY, G.I.; DUCAS, J.D.; CUSTÓDIO, A.P.; PINTO, M.A.; MENDES, A.A. 2016. Interfacial activation of lipases on hydrophobic support and application in the synthesis of a lubricant ester. *Internal J. Biological Macromolecules*. 92:900-909. <https://doi.org/10.1016/j.ijbiomac.2016.07.097>
- BASTIDA, A.; SABUQUILLO, P.; ARMISEN, P.; FERNÁNDEZ-LAFUENTE, R.; HUGUET, J.; GUISÁN, J.M. 1998. A single step purification, immobilization, and hyperactivation of lipases via interfacial adsorption on strongly hydrophobic supports. *Biotechnology and Bioengineering*. 58(5):486-493. [https://doi.org/10.1002/\(SICI\)1097-0290\(19980605\)58:5<486::AID-BIT4>3.0.CO;2-9](https://doi.org/10.1002/(SICI)1097-0290(19980605)58:5<486::AID-BIT4>3.0.CO;2-9)
- BERNAL, C.; POVEDA-JARAMILLO, J.C.; MESA, M. 2018. Raising the enzymatic performance of lipase and protease in the synthesis of sugar fatty acid esters, by combined ionic exchange-hydrophobic immobilization process on aminopropyl silica support. *Chemical Engineering J*. 334:760-767. <https://doi.org/10.1016/j.cej.2017.10.082>
- CIPOLATTI, E.P.; VALÉRIO, A.; NINOW, J.L.; DE OLIVEIRA, D.; PESSELA, B.C. 2016. Stabilization of lipase from *Thermomyces lanuginosus* by crosslinking in PEGylated polyurethane particles by polymerization: Application on fish oil ethanolysis. *Biochemical Engineering J*. 112:54-60. <https://doi.org/10.1016/j.bej.2016.04.006>
- ESCOBAR, S.; BERNAL, C.; BOLIVAR, J.M.; NIDETZKY, B.; LÓPEZ-GALLEGO, F.; MESA, M. 2018. Understanding the silica-based sol-gel encapsulation mechanism of *Thermomyces lanuginosus* lipase: The role of polyethylenimine. *Molecular Catalysis*. 449:106-113. <https://doi.org/10.1016/j.mcat.2018.02.024>
- FERENC, W.; CRISTÓVÃO, B.; SARZYŃSKI, J.; SADOWSKI, P. 2012. Complexes of the selected transition metal ions with 4-methoxycinnamic acid: Physico-chemical properties. *J. Thermal Analysis and Calorimetry*. 110(2):739-748. <https://doi.org/10.1007/s10973-011-1935-5>
- FERNANDEZ-LAFUENTE, R. 2010. Lipase from *Thermomyces lanuginosus*: Uses and prospects as an industrial biocatalyst. *J. Molecular Catalysis B: Enzymatic*. 62(3):197-212. <https://doi.org/10.1016/j.molcatb.2009.11.010>
- FERNANDEZ-LORENTE, G.; CABRERA, Z.; GODOY, C.; FERNANDEZ-LAFUENTE, R.; PALOMO, J.M.; GUISÁN, J.M. 2008. Interfacially activated lipases against hydrophobic supports: Effect of the support nature on the biocatalytic properties. *Process Biochemistry*. 43(10):1061-1067. <https://doi.org/10.1016/j.procbio.2008.05.009>
- HANSON, K.M.; NARAYANAN, S.; NICHOLS, V.M.; BARDEEN, C.J. 2015. Photochemical degradation of the UV filter octyl methoxycinnamate in solution and in aggregates. *Photochemical and Photobiological Sciences*. 14(9):1607-1616. <https://doi.org/10.1039/c5pp00074b>

11. HOLSER, R.A. 2008. Kinetics of cinnamoyl glycerol formation. *JAOCS, J. the American Oil Chemists' Society.* 85(3):221-225.
<https://doi.org/10.1007/s11746-007-1189-3>
12. HOLSER, R.A.; MITCHELL, T.R.; HARRY-O'KURU, R.E.; VAUGHN, S.F.; WALTER, E.; HIMMELSBACH, D. 2008. Preparation and Characterization of 4-Methoxy Cinnamoyl Glycerol. *J. American Oil Chemists' Society.* 85(4):347-351.
<https://doi.org/10.1007/s11746-008-1197-y>
13. KATZ, L.M.; DEWAN, K.; BRONAUGH, R.L. 2015. Nanotechnology in cosmetics. *Food and Chemical Toxicology.* 85:127-137.
<https://doi.org/10.1016/j.fct.2015.06.020>
14. KUO, S.-J.; PARKIN, K.L. 1996. Solvent polarity influences product selectivity of lipase-mediated esterification reactions in microaqueous media. *J. American Oil Chemists' Society.* 73(11):1427-1433.
<https://doi.org/10.1007/BF02523507>
15. LEE, C.H.; PARKIN, K.L. 2001. Effect of water activity and immobilization on fatty acid selectivity for esterification reactions mediated by lipases. *Biotechnology and Bioengineering.* 75(2):219-227.
<https://doi.org/10.1002/bit.10009>
16. LEE, G.S.; WIDJAJA, A.; JU, Y.H. 2006. Enzymatic synthesis of cinnamic acid derivatives. *Biotechnology Letters.* 28(8):581-585.
<https://doi.org/10.1007/s10529-006-0019-2>
17. MATTE, C.R.; BUSSAMARA, R.; DUPONT, J.; RODRIGUES, R.C.; HERTZ, P.F.; AYUB, M.A.Z. 2014. Immobilization of *Thermomyces lanuginosus* lipase by different techniques on Immobead 150 support: Characterization and applications. *Applied Biochemistry and Biotechnology.* 172(5):2507-2520.
<https://doi.org/10.1007/s12010-013-0702-4>
18. MONSALVE, Y.; SIERRA, L.; LÓPEZ, B.L. 2015. Preparation and characterization of succinyl-chitosan nanoparticles for drug delivery. *Macromolecular Symposia.* 354(1):91-98.
<https://doi.org/10.1002/masy.201400128>
19. NAIK, S.; BASU, A.; SAIKIA, R.; MADAN, B.; PAUL, P.; CHATERJEE, R.; BRASK, J.; SVENDSEN, A. 2010. Lipases for use in industrial biocatalysis: Specificity of selected structural groups of lipases. *J. Molecular Catalysis B: Enzymatic.* 65:18-23.
<https://doi.org/10.1016/j.molcatb.2010.01.002>
20. NOHYNEK, G.J.; DUFOUR, E.K. 2012. Nano-sized cosmetic formulations or solid nanoparticles in sunscreens: A risk to human health? *Archives of Toxicology.* 86(7):1063-1075.
<https://doi.org/10.1007/s00204-012-0831-5>
21. PALACIO, J.; MONSALVE, Y.; RAMÍREZ-RODRÍGUEZ, F.; LÓPEZ, B. 2020. Study of encapsulation of polyphenols on succinyl-chitosan nanoparticles. *J. Drug Delivery Science and Technology.* 57:101610.
<https://doi.org/10.1016/j.jddst.2020.101610>
22. PATIL, D.; DEV, B.; NAG, A. 2011. Lipase-catalyzed synthesis of 4-methoxy cinnamoyl glycerol. *J. Molecular Catalysis B: Enzymatic.* 73(1-4):5-8.
<https://doi.org/10.1016/j.molcatb.2011.07.002>
23. SAHATSAPAN, N.; ROJANARATA, T.; NGAWHIRUNPAT, T.; OPANASOPIT, P.; PATROJANASOPHON, P. 2019. Catechol-functionalized succinyl chitosan for novel mucoadhesive drug delivery. *Key Engineering Materials.* 819:21-26.
<https://doi.org/10.4028/www.scientific.net/KEM.819.21>
24. SANTOS, A.C.; MORAIS, F.; SIMÕES, A.; PEREIRA, I.; SEQUEIRA, J.A.D.; PEREIRA-SILVA, M.; VEIGA, F.; RIBEIRO, A. 2019. Nanotechnology for the development of new cosmetic formulations. *Expert Opinion on Drug Delivery.* 16(4):313-330.
<https://doi.org/10.1080/17425247.2019.1585426>
25. SHAATH, N.A. 2010. Ultraviolet filters. *Photochem. Photobiol. Sci.* 9(4):464-469.
<https://doi.org/10.1039/B9PP00174C>
26. SOTO, I.D.; ESCOBAR, S.; MESA, M. 2017. Study of the physicochemical interactions between *Thermomyces lanuginosus* lipase and silica-based supports and their correlation with the biochemical activity of the biocatalysts. *Materials Science and Engineering C.* 79:525-532.
<https://doi.org/10.1016/j.msec.2017.05.088>
27. SUN, W.J.; ZHAO, H.X.; CUI, F.J.; LI, Y.H.; YU, S.L.; ZHOU, Q.; QIAN, J.Y.; DONG, Y. 2013. D-isoascorbyl palmitate: Lipase-catalyzed synthesis, structural characterization and process optimization using response surface methodology. *Chemistry Central J.* 7(1):1-13.
<https://doi.org/10.1186/1752-153X-7-114>
28. YESILOGLU, Y.; KILIC, I. 2004. Lipase-Catalyzed Esterification of Glycerol and Oleic Acid. *JAOCS, J. American Oil Chemists' Society.* 81(3):281-284.
<https://doi.org/10.1007/s11746-004-0896-5>
29. ZHANG, C.-G.; ZHU, Q.-L.; ZHOU, Y.; LIU, Y.; CHEN, W.-L.; YUAN, Z.-Q.; YANG, S.-D.; ZHOU, X.-F.; ZHU, A.-J.; ZHANG, X.-N.; JIN, Y. 2014. N-succinyl-chitosan nanoparticles coupled with low-density lipoprotein for

targeted osthole-loaded delivery to low-density lipoprotein receptor-rich tumors. *International J. Nanomedicine*. 9(1):2919-2932.
<https://doi.org/10.2147/IJN.S59799>

30. ZHOU, Z.; INAYAT, A.; SCHWIEGER, W.; HARTMANN, M. 2012. Improved activity and stability of lipase immobilized in cage-like large pore mesoporous organosilicas. *Microporous and Mesoporous Materials*. 154:133-141.
<https://doi.org/10.1016/j.micromeso.2012.01.003>